BioNanoScience (2022) 12:571–581
https://doi.org/10.1007/s12668-022-00949-3

RESEARCH ARTICLE

Magnetic Field Effect on the Magnetic Nanoparticles Trajectories in Pulsating Blood Flow: a Computational Model

Laura Mańia Roa-Barrantes[1] · Diego Julián Rodriguez Patarroyo[1]

Accepted: 6 February 2022 / Published online: 25 March 2022

Abstract

Magnetic drug targeting is a non-invasive biomedical technique for the treatment of localized diseases. This technique is based on the bonding of the drug to the nanoparticles' surface with a magnetizable core, suspended in a liquid known as ferrofluid that is injected into the bloodstream and directed to the target region through external magnetic fields. In this article, the kinetic behavior of a magnetic nanoparticle subjected to external magnetic fields at four moments of the cardiac cycle is compared to understand the dynamic effect due to the blood pulsating. For it, a 100 μm diameter non-bifurcated and radially symmetrical blood vessel is approximated with pulsating flux and a 100 nm radius magnetic nanoparticle, driven by external magnetic fields associated with a cylindrical neodymium magnet. Two forces are taken into account: the magnetic force on the nanoparticle and the drag force influenced by the velocity profiles of the blood flow as well as its velocity. The effects of gravity and thermal are not taken into account. In the results, a proportional relationship was obtained between the shape of the velocity profile caused by the moment of the cardiac cycle with the trajectories of the nanoparticles, where capture in the early and late cardiac relaxation phase is facilitated.

Keywords Blood velocity profiles · Magnetic drug targeting · Magnetic nanoparticles · Particle trajectory

1 Introduction

Magnetic drug targeting (MDT) is a growing biomedical technique that can provide new opportunities to improve the quality of life of patients exposed to aggressive pharmacological treatments, preventing them from reaching all tissues indiscriminately, which can reduce adverse effects. as unnecessary cell death [1, 2]. In this technique, a ferrofluid is injected into the blood vessels near the area of interest, and its trajectories are directed by external magnetic fields [2–4], which occurs in this case by a permanent cylindrical magnet close to 0, 4 T superficial (NdFeB) [5–7] A ferromagnetic fluid is a colloidal suspension of magnetic nanoparticles (MNP) with individual magnetic moments dispersed in a carrier liquid or matrix [8, 9]. To avoid agglomerations, reduce toxicity and facilitate drug transport, the magnetic core nanoparticles, commonly made of magnetite (Fe_3O_4) and high magnetic susceptibility [10], are coated with a porous biocompatible material capable of transporting the drug [8]. One of the most common NPM synthesis methods is chemical precipitation, where, in general, iron II and III chloride are mixed with ammo- nium hydroxide, then they undergo different peptization processes, that is, a colloidal suspension is created. Finally, using a cold solvent, the magnetic separation and the dissolution of the ferrofluid are carried out in such a way that spherical MNPs that can have from 10 nm onwards are obtained [8, 10].

One of the factors that affect the trajectory of MNPs is the cardiac cycle since they are injected directly into arterioles that feed the target site. It is known that the deformation rates can cause changes in viscosity due to the characteristics of the cardiac cycle, the size, and elasticity of the walls of the blood vessels [11–13]; it has also been shown, employing microvasculature models, that no significant differences are found in the variation of viscosity and arterial pressure in areas where the vessels are uniform and without bifurcations. Therefore, the transport of MNPs through short sections of the arterioles

Diego Julián Rodriguez Patarroyo contributed equally to this work.

✉ Laura Mańia Roa-Barrantes
lmroab@correo.udistrital.edu.co

Diego Julián Rodriguez Patarroyo
djrodriguezp@udistrital.edu.co

[1] Engineer Faculty, Universidad Distrital Francisco Jośe de Caldas, Bogotá, Colombia

is influenced by the velocity profiles of blood flow at the arteriolar level, which in turn depends on the nature of the cardiac cycle and the characteristics of the blood fluid as a Newtonian fluid [11, 13].

Some authors have proposed different ways of approaching the computational study of the MDT technique, taking into account different characteristics of the system such as the size of the blood vessel, the viscosity of the fluid, the cell aggregates, the quantity, and size of the MNP [14, 15]. The proposals aim to solve the Navier-Stokes equations, commonly making use of numerical methods using techniques such as differences or finite elements [16]. On the other hand, the classical molecular dynamics (MD) technique is used to solve the equations, where the movement of each of the MNPs involved in the system is studied [17]. The purpose of classical DM can be understood as the time-dependent study of the behavior of microscopic systems. DM seeks to predict how a system of particles will move from the equations of motion, in some non-linear cases, by numerical integration [18, 19]. The solution of these equations allows predicting the trajectory of the magnetic nanoparticles with a low computational cost compared to other solutions such as those of finite elements [17].

In particular, previous works such as that of Haverkort et al. [16], they apply the MDT technique in large human arteries (left coronary artery), taking into account the characteristics of the blood flow. This is through 3D simulations to capture MNP. They find that 50% of them are captured by the magnetic field due to the high speed of blood flow in these types of vessels. Lunnoo et al. [20] computationally studied the capture efficiency based on the size of the iron nanoparticles, magnetite, and maghemite core, as well as the effects of different coatings as a drug-carrying structure. In their findings, they describe that the coating has a negligible influence on the magnetization of the nanoparticle, as well as the appropriate size of the magnetic core between 10 and 200 nm. They conclude that the efficiency of capturing the particles decreases as their size is reduced. Furlani and Ng. [21] developed an analytical method to predict transport and MNP capture, with a magnetic field, for which they affirm that malignant tissue can be located within the body several centimeters away as long as the magnetic field is strong enough. Then, Furlani and Furlani [22] mathematically predict the MNP transport, using analytical methods. Finally, they suggest that the theory developed can be used to optimize the particle size as well as the parameters of the external magnet, taking into account the magnetic field of this, the drag force and the magnetization of the particle. Sharma et al. [23] developed a mathematical model which predicts the trajectories of a group of MNPs; they found the solution of the equations using the Runge-Kutta method of order four. They affirm that the total of the nanoparticles in the center of the magnet was captured, only when it is very close to the body, and that as it moves away, the capture decreases to zero. Mahmoodpour et al. [15] investigated, using finite-element method computational simulation, the MNP trajectories in venous vessels with a diameter of 1 cm in two cases, first with uniform distribution of nanoparticles into the body. Second, injecting them close to the target region, finding that the MNP capture efficiency improves by 85% when injected near the target area. Rodriguez-Patarroyo and Roa. Barrantes [24, 25] propose a computational simulation which allows predicting the path of MNP in two conditions: initially assuming a straight blood vessel with arteriole characteristics and a constant laminar flow. Second, the cellular aggregates that collide with the nanoparticles are also taken into account. In their findings, the nanoparticles reach the target region while under the influence of the magnetic field, so that the optimized distance between the center of the blood vessel and the magnet is between 1.8 and 2.2 cm.

This article studied the magnetic targeting of a magnetic nanoparticle in an arteriole with pulsatile flow. A single MNP is found because the nanoparticle density of the ferrofluid is low enough to avoid clustering processes. In Fig. 1, an approximation to the physical system is represented.

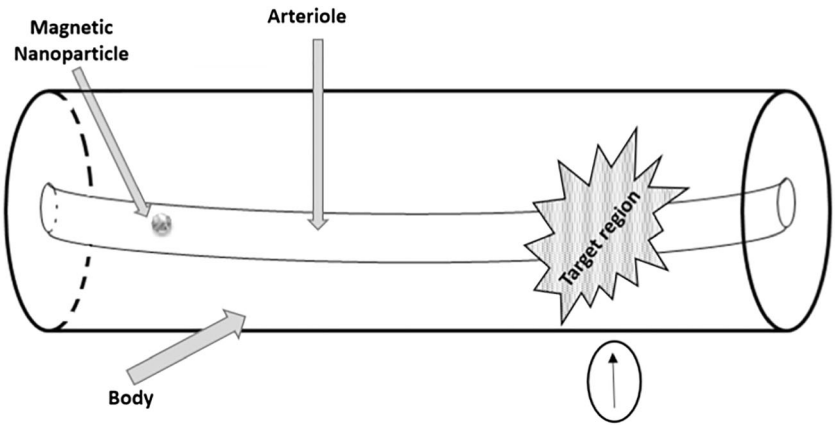

Fig. 1 MNP transport system scheme

2 Methodology

The magnetic transport of a nanoparticle in the microvascular system is governed by several factors. The magnetic force $\mathbf{F}_m$ produced by the external magnetic field **H** and the force of drag the drag force of the blood flow $\mathbf{F}_f$ influenced by the cardiac cycle. The blood flow was taken as a pulsating laminar flow and of constant apparent viscosity. The coordinate system is taken two-dimensional due to the cylindrical symmetry of the vessel, so the radial direction is taken as Q and the longitudinal or blood flow direction as z, as can be seen in Fig. 2. Additionally, velocity profiles were determined at four moments of the cardiac cycle as can be seen in Fig. 3, where it is evident how the velocity profile depends on the contraction or relaxation of the heart (diastole or systole). In Tables 1, 2, the parameters used are based on the literature [14, 20, 21, 26]; the nomenclature used is presented.

2.1 Model

To find the equations that allow predicting the trajectories of the MNP, initially, the magnetic force produced by the external magnet on the MNP is determined, then the drag force caused by the average velocity of the blood is found, and the velocity profile that varies in every moment of the cardiac cycle.

2.1.1 Magnetic Force

The nanoparticles trajectories are influenced by the external magnetic field, which while it is present, it magnetizes each nanoparticle as a superparamagnetic mono-domain that in turn responds kinetically in the direction of the same and, once it is removed, the magnetic core of the nanoparticle loses its magnetization, making it less harmful for biological use [6, 7]. Table 2 describes the characteristics assumed for the permanent magnet and the nanoparticle.

The Eqs. 1 and 2 correspond to the magnetic field produced by the infinite cylindrical magnet that is magnetized perpendicular to its axis, the components in each axis (Q, y, z) can be represented inside the vessel as follows:

$$H_q(z,Q) = \frac{M_s R_m^2}{2} \frac{(Q+d)^2 - z^2}{\left[(Q+d)^2 + z^2\right]^2} \tag{1}$$

$$H_z(z,Q) = \frac{M_s R_m^2}{2} \frac{2(Q+d)z}{\left[(Q+d)^2 + z^2\right]^2} \tag{2}$$

The Eqs. 3 and 4 represent the magnetic force in each of the axes (Q and z), which is exerted on the nanoparticle, which presents an attractive response when entering the magnetic field produced by the external magnet.

$$\mathrm{F}_{mq}(z,Q) = C_1 \frac{d}{2\left[d^2 + z^2\right]^3} \tag{3}$$

$$\mathrm{F}_{mz}(z,Q) = C_1 \frac{z}{2\left[d^2 + z^2\right]^3} \tag{4}$$

where C_1 is the constant: $3\mu_0 v_p M^2 R^4$,resulting from taking into account the characteristics of the nanoparticle and the magnet; among them are the radius of the magnet, magnetic permeability in a vacuum, the volume of the particle, the radius and magnetization of the MNP [14, 15].

2.1.2 Drag Force on the Nanoparticle

A pulsating laminar fluid parallel to the z-axis with constant apparent viscosity is approximated in a cylindrical blood vessel with a radius of 50 μm. Table 2 shows the parameters considered for both flow and blood vessel, and Fig. 3 shows the four velocity profiles taken during the cardiac cycle.

The drag force on the nanoparticle can be expressed as shown in the Eq. 5, where F_0 corresponds to $6\pi\eta R_p$. The velocities of the nanoparticle and the average flow velocity are $\mathbf{V}_p$ and $\overline{\mathbf{V}}_f$ respectively.

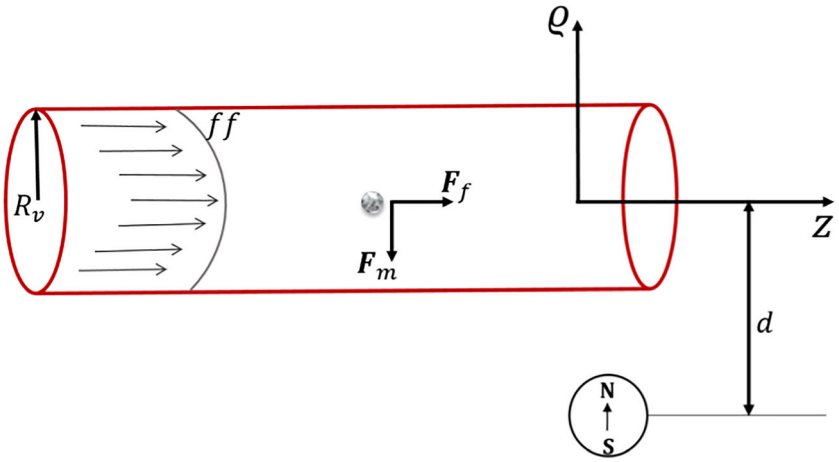

Fig. 2 MNP transport reference system

Table 1 Parameters and features

Parameter	Value	Unit	Reference
Permanent magnet			
Material	Rare earths	NdFeB	[21]
Diameter	$4 \leq d \leq 6$	cm	[14]
Magnetic Saturation	10^6	$A\ m^{-1}$	[16]
Magnetic nanoparticle			
Material	Fe_3O_4	Magnetite	[14]
Diameter	$75 \leq d \leq 200$	nm	[20]
Susceptibility	$\chi >> 1$	–	[14]
Density	$5000 \geq \rho \geq 6450$	Kgm^{-3}	[7]
			[14]
Vessel and blood flow			
Radius	$50 \leq R \leq 75$	$\mu\ m$	[22]
Viscosity	$3.2 * 10^{-3}$	$Ns\ m^{-2}$	[14]
Density	1060	$Kg\ m^{-3}$	[14]
			[16]
Average velocity	10	$mm\ s^{-1}$	[14]
Shape factor (velocity profile)	$0.1 \leq \zeta \leq 1.3$	–	Own

Table 2 Nomenclature

$\mathbf{F}_m$	Magnetic force (N)	$\mathbf{F}_f$	Drag force (N)
Ms	Magnetization (Am^{-1})	Rm	Magnet radius
μ_0	Vacuum permeability (NA^{-2})	η	Blood viscosity (Nsm^{-2}) Rp
R_p	Nanoparticle radius (nm)	ζ	Velocity profile shape factor d
d	Blood-vessel and magnet distance	$\mathbf{H}$	External magnetic field

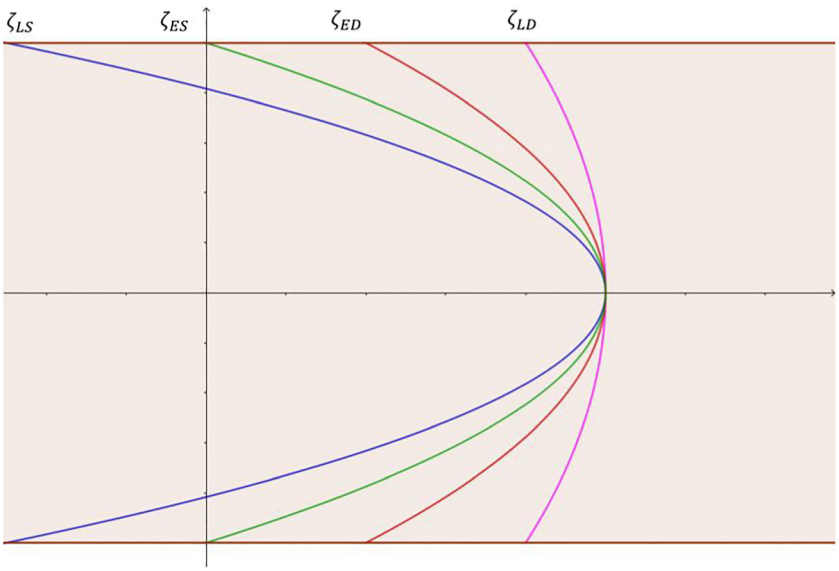

Fig. 3 Cardiac cycle velocity profiles: in **magenta** late diastole (ζ_{LD}), in **red** early diastole (ζ_{ED}), in **green** early systole (ζ_{ES}) and, in **blue** late systole (ζ_{LS})

$$\mathrm{F}_f = -F_0\left(\mathbf{V}_p - \overline{\mathbf{V}}_f\right) \tag{5}$$

The final velocity of the nanoparticle depends on $\overline{\mathbf{V}}_f$ and the velocity profile given in this case of parabolic shape, as shown in the Eq. 6. The factor that precedes the quadratic function (ζ) gives the attenuated or steep parabolic shape of the velocity profile.

$$\mathrm{V}_f = 2\overline{\mathbf{V}}_f 1 - \zeta\frac{Q}{R_v}^{2^{\#}} \tag{6}$$

Therefore, the drag force results as can be seen in the Eqs. 7 and 8 for the axes Q and z respectively.

$$\mathrm{F}_{fq} = -F_0\mathbf{V}_{pq} \tag{7}$$

$$\mathrm{F}_{fz} = -F_0\mathbf{V}_{pz} - 2\overline{\mathbf{V}}_f 1 - \zeta\frac{Q}{R_v}^{2^{\#\#}} \tag{8}$$

Four velocity profiles were taken into account, Eq. 9 shows an early diastole with a form factor ($\zeta = 0.6$) and a late diastole ($\zeta = 0.2$), in Eq. 10 shows an early systole ($\zeta = 1.0$) and a typical parabolic profile of a late systole ($\zeta = 1.3$), with retrograde flow in the vessel walls.

$$1 - 0.6\frac{Q}{R_v}^{2^{\#}} 1 - 0.2\frac{Q}{R_v}^{2^{\#}} \tag{9}$$

MDT in pulsating blood flow

$$1 - 1.0\frac{Q}{R_v}^{2^{\#}} 1 - 1.3\frac{Q}{R_v}^{2^{\#}} \tag{10}$$

As a result of applying Newton's equations, the equations of motion 11 and 12 are obtained that predict the trajectories of the nanoparticles.

$$\frac{d\mathrm{V}_{pq}}{dt} = \frac{C_2}{m}\frac{d}{2\left(d^2+z^2\right)^3} - \frac{F_0}{m}\mathbf{V}_q \tag{11}$$

$$\frac{d\mathrm{V}_{pz}}{dt} = \frac{2F_0\overline{\mathbf{V}}_f}{m}\frac{C_2}{m} \quad 1 - \zeta\frac{Q}{R_v}^{2^{\#}} + \frac{C_2}{m}\frac{z}{\left(d^2+z^2\right)^3} - \frac{F_0}{m}\mathbf{V}_z \tag{12}$$

where C_2 is the constant $\mu_0 R^2 M^2 R^4$, d is the distance between the magnet and the center of the blood vessel, and F_0 corresponds to the drag force of the fluid, determined by $6\pi\eta R_p\mathbf{V}_{pq}$.

2.1.3 Numerical Method

In this study, the equations that model nanoparticles trajectories are non-linear second-order partial differential equations. the solution to these equations is carried out using the molecular dynamics technique. This is a first-principles technique that simulates trajectories step by step. In particular, the DM is advanced in time, repeatedly calculating the forces in each MNP and then using those forces to update the position and speed of each one [18, 19, 27]. The purpose of MD is to understand and predict how a particle system will move in time, to understand physiological phenomena, through the numerical solution of equations of motion.

To calculate the displacement evolution that describes the nanoparticle trajectories, it implemented an algorithm in C^{++} sensitive to initial conditions as can be seen in Table 2. Both position and velocity parameters were defined that were significant in the modeling and study of the behavior of the particle. With MD simulations, time-dependent phenomena can be studied.

3 Results and Discussion

Graphs show the MNP at the origin coordinate system of the blood vessel; therefore, the radius is represented on the Q-axis from the center of the vessel (0 m) to the wall proximal to the magnet (50^{-6} m), where the magnetic field act, and the MNP initially is situated at 3 cm on the z-axis as can be seen in Fig. 2. From the modifications of ζ in the equations of motion, the velocity profiles observed in Fig. 4 are obtained as a representative, based on studies carried out by [28, 29]: for the profile $\zeta = 0.6$, early diastole, a shallow parabolic profile is obtained due to the initial distension of the blood vessels and, consequently, the cross-sectional area begins to increase. The profile $\zeta = 0.2$ called late diastole is almost flat since at this moment in the cardiac cycle the heart and arteries are relaxed; in the center of the vessel, the profile is not very pronounced, since the aqueous phase of the blood (plasma) remains with the remnant of the drag force of the immediately previous cycle, thus allowing a constant flow to the organs that require it. The $\zeta = 1.0$ profile represents early systole; it is the moment of ventricular contraction when the blood flow is pushed in the z-direction and, therefore, a prominent parabolic curve is observed. Finally, the profile corresponds to late systole, when the contraction ends, besides, adhesion of the blood plasma to the arterial walls provides a retrograde flow towards the walls and a very pronounced parabolic profile in the center of the vessel.

Figure 5 shows nanoparticle position both on the radial axis (Q) and on the axis of the blood flow direction (z) when it is under different magnetic fields at the cause of the variation in d. The distance values 1.8 d 2.2 cm are taken from previous works ([25]) where the optimal range for nanoparticle capture was determined, for this group of parameters. Additionally, the value of $d = 2.3$ cm was taken to observe the changes in the trajectories even if the MNPs are not captured. It can be seen in the Fig. 5a (d = 1.8 cm) that the trajectories very little

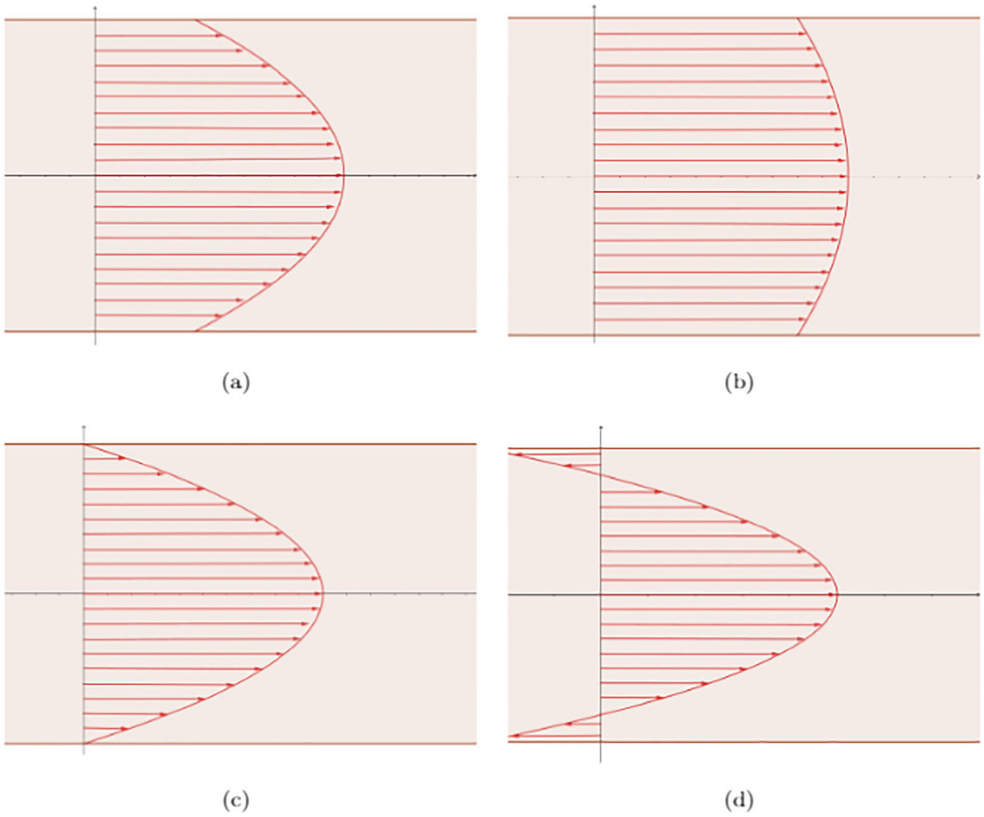

Fig. 4 Velocity profiles during the cardiac cycle: **a** early diastole ($\zeta = 0.6$); **b** late diastole ($\zeta = 0.2$); **c** early systole ($\zeta = 1.0$); **d** late systole ($\zeta = 1.3$)

perceptibly in each of the velocity profiles since they are captured towards the center of the magnet, being consistent with the optimized value according to [25]. Figure 5b ($d = 2.0$ cm) shows all the trajectories of the nanoparticles as well as the captures of the MNPs from the center towards the distal part of the permanent magnet; the variation of the capture position is evident according to the speed profile evaluated. While in Fig. 5c ($d = 2.2$ cm), the trajectories are affected by the curvature of the velocity profile, that is, being in early diastole when the influence of the magnetic field tends to zero and the drag force of the blood flow takes the MNPs in the z-direction; something similar happens in early systole, when the drag force is even greater than the attraction produced by the magnetic field, until the distance in Q is shortened to the magnet, so the drag force loses its effect on the MNP, generating an attraction towards the target region. In Fig. 5d ($d = 2.3$ cm), it is observed how the magnetic field deflects the trajectories of the MNP, where the effect of the attractive force tends to zero compared to the drag force. It can also be observed that, in late systole, where retrograde flow occurs, the drag force contributes to the return of the MNP for capture.

In Fig. 6, the position of the MNP is shown concerning the time it takes to be captured. An increase in speed can be observed as the intensity of the magnetic field increases, that is, as the distance of the magnet regarding the MNP decreases. A small difference in the velocities concerning the blood flow velocity profiles is evident in Fig. 6a and b, since in most cases the MNP is captured before 6 ms; In the particular case of a magnet distance of 1.8 cm, it is evident that regardless of the velocity profile of the blood, the quickness with which the MNP has captured increases significantly. Regarding the speed with which the trajectories of the MNP vary when they are under a weaker field ($d = 2.3$ cm), a smaller slope is observed, which indicates that the magnetic attraction force is ineffective to modify the position of the MNP and therefore, the drag force predominates, taking them in the z-direction.

Figures 7 and 8 show the nanoparticles trajectories in different initial conditions along the Q-axis at different times of the cardiac cycle for $d = 1.8$ and $d = 2.3$ cm. It is observed how the shape of the velocity profile, of the blood flow, significantly influences the trajectory, in the case of late systole (in blue color) in the Fig. 8, as a result of the retrograde flow, the MNP they are captured only when they approach the wall of the blood vessel closest to the magnet; otherwise, the drag force will be greater and the MNP will continue in the z-direction.

Taking into account the results obtained and that, in physiological terms, the heart rate of a healthy adult is approximately 70 bpm, that is, on average the cycle takes 1.25 Hz or 800 ms; additionally, this time is not distributed proportionally, since diastole takes about 500 ms and systole, being faster,

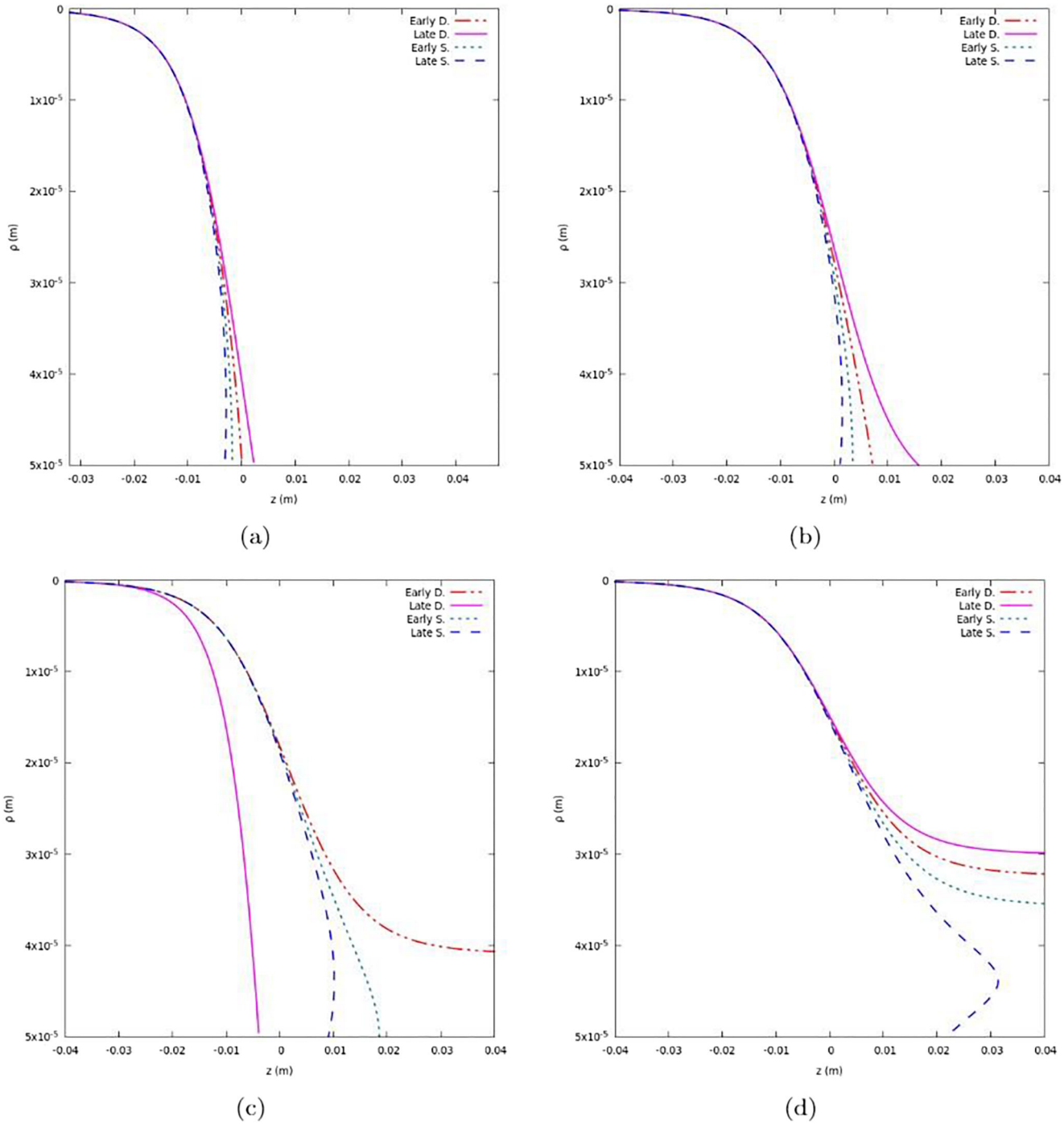

Fig. 5 Nanoparticle trajectories in each of the velocity profiles with the modification of the magnetic intensity: **a***d* = 1.8 cm; **b***d* = 2.0 cm; **c***d* = 2.2 cm; **d***d* = 2.3 cm

takes 300 ms [30]. Therefore, it can be affirmed that the MNP capture efficiency is higher during late diastole and early systole; this due to the fact that the velocity profile is less pronounced, in other words, the drag force decreases compared to the other profiles.

When comparing the results obtained in the static case with previous studies [25], that is, without taking into account the influence of the velocity profile on the MNP trajectory. An increase in the nanoparticles dispersion is evidenced, with the cardiac cycle being a source of the reduction in efficiency in the MDT technique. These findings may guide future works involving additional conditions that may affect the capture efficiency of MNPs, such as arteriolar topology with bifurcations, interaction with formed elements such as erythrocytes or changes in pressure and temperature.

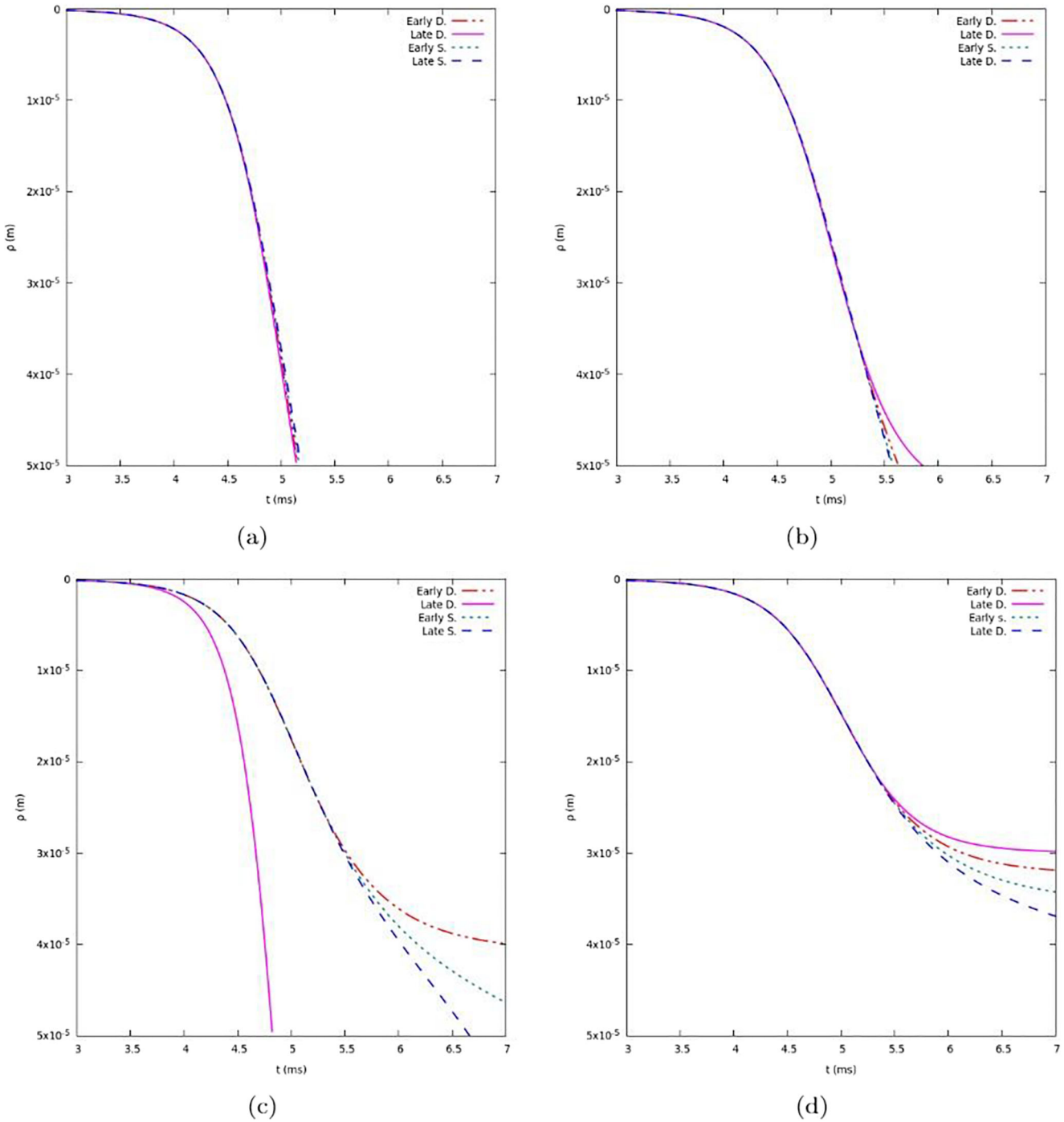

Fig. 6 MNP velocity in each of the velocity profiles with variation of the magnetic intensity: **a***d* = 1.8 cm; **b***d* = 2.0 cm; **c***d* = 2.2 cm; **d***d* = 2.3 cm

In the work of Mahmoodpour et al. [15], they conclude that introducing MPNs into venous blood vessels (without pulsations) implies that they must pass through the bloodstream at high speed to be captured by the magnet. When contrasting the results obtained, it can be affirmed that including the pulsatile factor of the blood flow allows showing at what moment of the cardiac cycle the injection of MPN is most recommended, given the behavior observed in the Figs. 7 and 8.

4 Conclusions

A mathematical model has been presented that, through computational simulation, allows predicting the kinetics of magnetic nanoparticles by the action of an external magnetic field, in a cylindrical blood vessel without bifurcations and pulsating flow. The model incorporates all the forces that significantly influence the nanoparticles' kinetics, including the drag

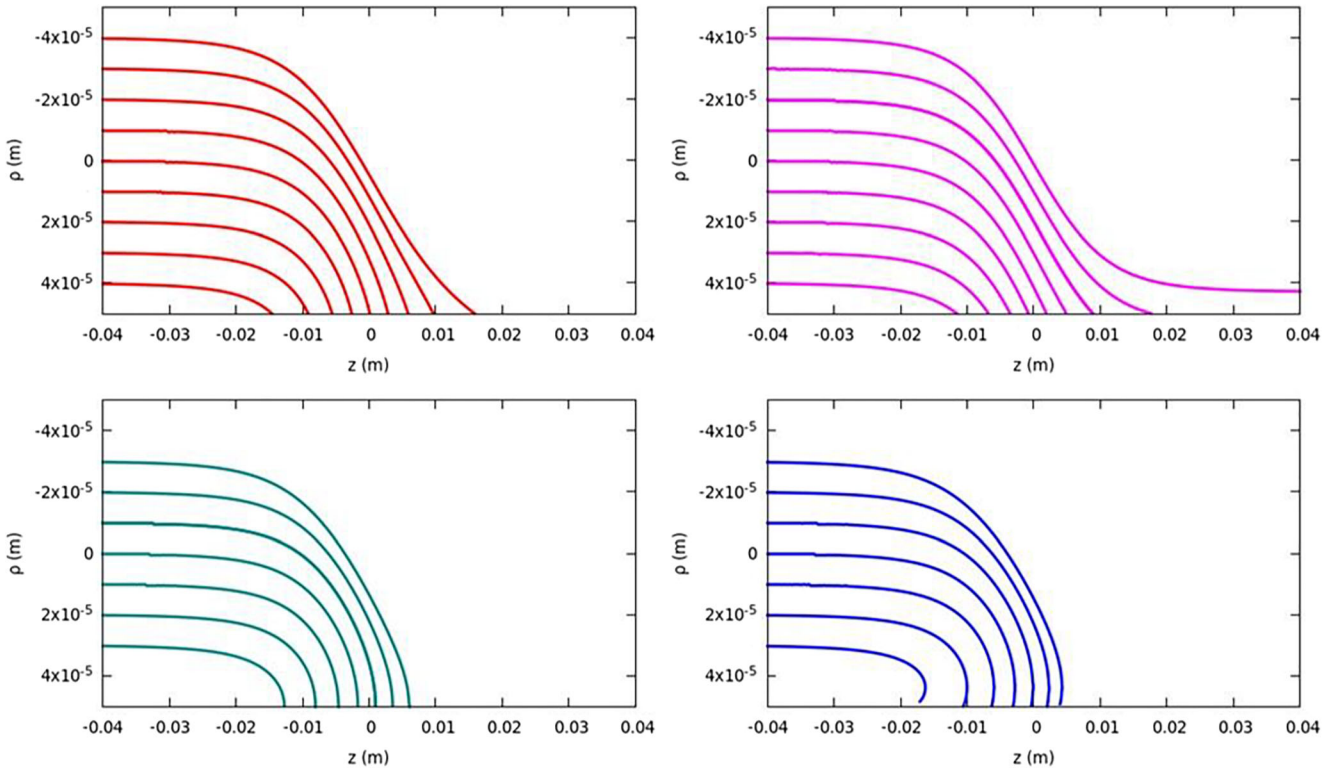

Fig. 7 MNP trajectories with starting position change on the ϱ-axis with the distance to the magnet d = 1.8 cm. The color indicates the cardiac cycle moment, in **red**: early diastole, **magenta**: late diastole, **cyan**: early systole and **blue**: late systole

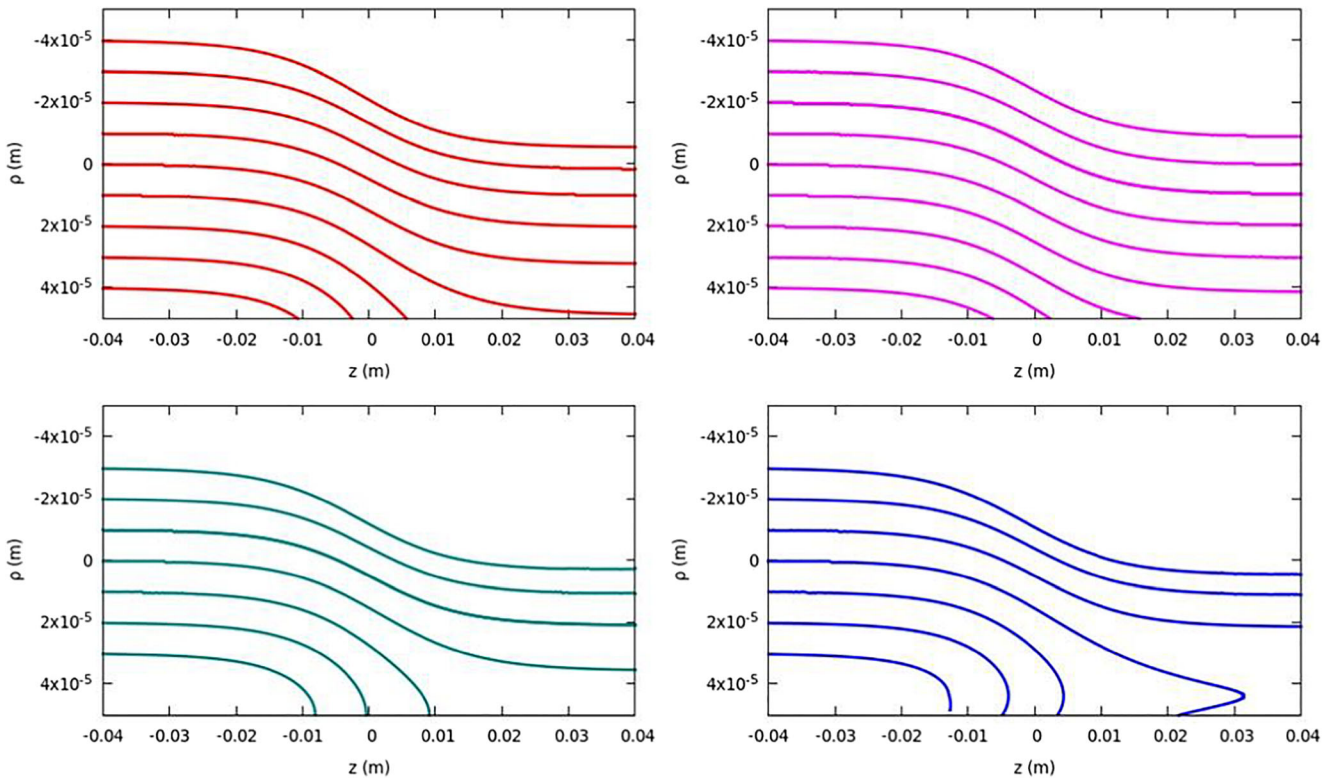

Fig. 8 MNP trajectories with starting position change on the ϱ-axis with the distance to the magnet d = 2, 3 cm. The color indicates the cardiac cycle moment, in **red**: early diastole, **magenta**: late diastole, **cyan**: early systole and **blue**: late systole

force at four moments of the cardiac cycle (diastole and systole, early and late for both cases). Presented work allows the understanding of the factors considered in the development of the mathematical model, including the moments of the cardiac cycle and its influence on the MPN trajectory.

Results show that the nanoparticles fall under the influence of the magnetic field, depending on two factors, first the distance between the magnet and the center of the blood vessel. Second, the moment of the cardiac cycle in which the system is, that is to say, of the type of velocity profile that the blood flow has. The influence of the cardiac cycle moment is crucial for the capture of nanoparticles since the different blood flow velocity profiles significantly influence the trajectories. It should be noted that above 2.2 cm, the nanoparticle capture is only effective if it coincides with the time of the late diastole cardiac cycle. Likewise, when the velocity profiles are pronounced parabolic, the capture only occurs with the magnet at a distance of less than 2.0 cm.

Finally, it can be affirmed that having clarity regarding the velocity profiles in the influence of the kinetics of magnetically directed nanoparticles, can contribute to improving the effectiveness of magnetized drug targeting techniques for the management of diseases that require treatments aggressive, such as cancer.

Funding We explicitly clarify that this research was not funded by any public or private entity.

Declarations All authors certify the originality and unpublished of the article, and declare that it has not been previously published, nor is it being submitted to another publication

Conflict of Interest None.

Research Involving Humans and Animals Statement None.

Informed Consent All authors we authorize the publication of this manuscript.

References

1. Lübbe, A. S., Alexiou, C., & Bergemann, C. (2001). Clinical applications of magnetic drug targeting. *Journal of Surgical Research, 95*(2), 200–206. https://doi.org/10.1006/jsre.2000.6030
2. Tietze, R., Zaloga, J., Unterweger, H., Lyer, S., Friedrich, R. P., Janko, C., Pöttler, M., Dürr, S., & Alexiou, C. (2015). Magnetic nanoparticle-based drug delivery for cancer therapy. *Biochemical and Biophysical Research Communications, 468*(3), 463–470. https://doi.org/10.1016/j.bbrc.2015.08.022
3. Yameen, B., Choi, W. I., Vilos, C., Swami, A., Shi, J., & Farokhzad, O. C. (2014). Insight into nanoparticle cellular uptake and intracellular targeting. *Journal of Controlled Release, 190*, 485–499. https://doi.org/10.1016/j.jconrel.2014.06.038
4. Bertrand, N., Wu, J., Xu, X., Kamaly, N., & Farokhzad, O. C. (2014). Cancer nanotechnology: The impact of passive and active targeting in the era of modern cancer biology. *Advanced Drug Delivery Reviews, 66*, 2–25. https://doi.org/10.1016/j.addr.2013.11.009
5. Maity, A. R., & Stepensky, D. (2015). Delivery of drugs to intracellular organelles using drug delivery systems: Analysis of research trends and targeting effi- ciencies. *International Journal of Pharmaceutics, 496*(2), 268–274. https://doi.org/10.1016/j.ijpharm.2015.10.053
6. Mohammad Ali Ne, S., Ghassemi, M., Shahidian, A., & Majid Ghas-semi Ghasemi, B. (2017). Numerical investigation of drug delivery to cancerous solid tumors by magnetic nanoparticles using external magnet. *Transport in Porous Media, 119*(2), 461–480. https://doi.org/10.1007/s11242-017-0893-1
7. Kenjerš, S. (2016). On recent progress in modelling and simulations of multi-scale transfer of mass, momentum and particles in bio-medical applications. *Flow, Turbulence and Combustion, 96*(3), 837–860. https://doi.org/10.1007/s10494-015-9669-2
8. Zhang, X., Sun, L., Yu, Y., Zhao, Y. (2019). Flexible ferrofluids: design and applications. https://doi.org/10.1002/adma.201903497
9. Scherer, C., & Figueiredo Neto, A. M. (2005). Ferrofluids: Properties and applications. *Brazilian Journal of Physics, 35*, 3 A. https://doi.org/10.1590/S0103-97332005000400018
10. Imran, M., Affandi, A. M., Alam, M. M., Khan, A., & Khan, A. I. (2021). Advanced biomedical applications of iron oxide nanostructures based ferrofluids. *Nanotechnology, 32*, 42. https://doi.org/10.1088/1361-6528/ac137a
11. Baskurt, O.K., Meiselman, H.J. (2003). Blood rheology and hemodynamics. https://doi.org/10.3233/bir-1971-8206
12. Suárez Bagnasco, M., Suárez-Ántola, R. (2016). Contribuciones al estudio de las posible consecuencias fisiológicas y fisiopatológicas de la acumulación axial de los elementos formes de l sangre. Segunda parte: discusión biomecánica ampliada. Technical report. https://www.researchgate.net/publication/303984824
13. Isufrán, J., Franck, N., Ubal, S., Di Paolo, J. (2018). Modelado y simulación com- putacional mediante mef de unidades microscópicas para fraccionamiento de tejido sangúneo humano. Asociacíon Argentina de Mecánica Computaciona XXXVI, 6–9
14. Sharma, S., Gaur, A., Singh, U., & Katiyar, V. K. (2015). Capture Efficiency of Magnetic nanoparticles in a tube under magnetic field. *Procedia Materials Science, 10*(Cnt 2014), 64–69. https://doi.org/10.1016/j.mspro.2015.06.026
15. Mahmoodpour, M., Goharkhah, M., & Ashjaee, M. (2020). Investigation on trajectories and capture of magnetic drug carrier nanoparticles after injection into a direct vessel. *Journal of Magnetism and Magnetic Materials, 497*(October 2019), 166065. https://doi.org/10.1016/j.jmmm.2019.166065
16. Haverkort, J. W., Kenjerš, S., & Kleijn, C. R. (2009). Computational simulations of magnetic particle capture in arterial flows. *Annals of Biomedical Engineering, 37*(12), 2436–2448. https://doi.org/10.1007/s10439-009-9786-y
17. Aristizabal Soto, D. (2015). Técnica de simulación por dinámica molecular para la nanoindentación y nanorayado de peĺiculas delgadas. Technical report
18. Hollingsworth, S. A., & Dror, R. O. (2018). Molecular Dynamics Simulation for All. *Cell Press*. https://doi.org/10.1016/j.neuron.2018.08.011
19. De Vivo, M., Masetti, M., Bottegoni, G., & Cavalli, A. (2016). Role of molecular dynamics and related methods in drug discovery. *Journal of Medicinal Chemistry, 59*(9), 4035–4061. https://doi.org/10.1021/acs.jmedchem.5b01684
20. Lunnoo, T., & Puangmali, T. (2015). Capture efficiency of biocompatible magnetic nanoparticles in arterial flow: a computer simulation for magnetic drug targeting. *Nanoscale Research Letters, 10*, 1. https://doi.org/10.1186/s11671-015-1127-5
21. Furlani, E. P., & Ng, K. C. (2006). Analytical model of magnetic nanoparticle transport and capture in the microvasculature. *Physical*

Review E Statistical, Nonlinear, and Soft Matter Physics. https://doi.org/10.1103/PhysRevE.73.061919
22. Furlani, E. J., & Furlani, E. P. (2007). A model for predicting magnetic targeting of multifunctional particles in the microvasculature. *Journal of Magnetism and Magnetic Materials, 312*(1), 187–193. https://doi.org/10.1016/j.jmmm.2006.09.026
23. Sharma, S., Katiyar, V. K., & Singh, U. (2015). Mathematical modelling for trajectories of magnetic nanoparticles in a blood vessel under magnetic field. *Journal of Magnetism and Magnetic Materials, 379*, 102–107. https://doi.org/10.1016/j.jmmm.2014.12.012
24. Rodŕıguez-Patarroyo, D. J., Moyano-Valbuena, J. A., & Roa-Barrantes, L. M. (2018). Estudio por dinámica molecular browniana de nanopartículas bajo efectos de campos magńeticos externos. *Revista ingenieros militares, 53*(9), 1689–1699. https://doi.org/10.1017/CBO9781107415324.004
25. Roa-Barrantes, L. M., Rodŕıguez-Patarroyo, D. J., & Pantoja-Benavides, J. F. (2019). Kinetic model of magnetic nanoparticles in the bloodstream under the influence of an external magnetic field. *Communications in Computer and Information Science, 1052*, 596–604. https://doi.org/10.1007/978-3-030-31019-6
26. Kayal, S., Bandyopadhyay, D., Mandal, T. K., & Ramanujan, R. V. (2011). The flow of magnetic nanoparticles in magnetic drug targeting. *RSC Advances, 1*(2), 238–246. https://doi.org/10.1039/c1ra00023c
27. Spreiter, Q., & Walter, M. (1999). Classical molecular dynamics simulation with the Velocity Verlet algorithm at strong external magnetic fields. *Journal of Computational Physics, 152*(1), 102–119. https://doi.org/10.1006/jcph.1999.6237
28. Simpson, M.M., Janna, W.S. (2009). Newtonian and non-Newtonian fluids: velocity profiles, viscosity data, and laminar flow friction factor equations for flow in a circular duct, pp 173–180. https://doi.org/10.1115/imece2008-67611
29. Jan Tangelder, G., Slaaf, D.W., Muijtjens, A.M., Arts, T., oude Egbrink, M.G., Reneman, R.S. Velocity profiles of blood platelets and red blood cells flowing in arterioles of the rabbit mesentery.
30. Hall, J.E., Hall, M.E. (2020). Elsevier Health Sciences